Submicron Silica/Polystyrene Composite Particles Prepared by a One-Step Sol–Gel Process

ARTICLE *in* CHEMISTRY OF MATERIALS · MARCH 2003

Impact Factor: 8.35 · DOI: 10.1021/cm020980h

Submicron Silica/Polystyrene Composite Particles Prepared by a One-Step Sol−Gel Process

Hanan Sertchook and David Avnir*

Institute of Chemistry, The Hebrew University of Jerusalem, Jerusalem 91904, Israel

Received November 14, 2002. Revised Manuscript Received February 14, 2003

We describe a convenient, one-step sol−gel route to composite polymeric organic−inorganic particles. The synthesis is based on performing the sol−gel polycondensation within a surfactant-stabilized emulsion of a solution of a polymer — polystyrene of various molecular weights — in tetraethoxysilane, with or without toluene, all dispersed in a basic ethanolic medium. The parameters that dictate the formation of the composite bicontinuous particles were explored and characterized by several methods including TEM, surface area and porosity measurements, high-resolution XPS, TGA, DSC, UV, and FTIR spectroscopies. The particles are obtained in monomodal distributions with diameters in the range of 200−500 nm, depending on the preparation conditions. The polystyrene phase is extractable, and when this extraction is carried out porous silica particles are obtained. Likewise, partial extraction leads to core−shell architecture. The particles were also found to be good carriers for entrapped dye molecules with no leaching. Because of the hybrid nature of the particles, both hydrophobic dyes (Sudan III and IV) and hydrophilic dyes (the cationic Nile blue A) can be entrapped, utilizing the hydrophobic/hydrophilic phases of this composite material, respectively.

1. Introduction

Composite submicron particles made of organic polymers and oxides such as silica have found applications in catalysis[1], chromatography[2], controlled release[3], optics,[4] as materials additives (fillers),[5] and in many other fields. Various methods have been developed for the preparation of these composite silica/organic polymers, including layer-by-layer deposition,[6] polymerization of organic monomers with silane-modified surfaces of latex particles followed by Si-alkoxide polycondensation,[7] polymerization of an organic monomer in the presence of silica particles,[8] and incorporation of colloidal silica particles within latex particles by spray drying[9] or covalent bonding methods.[10] When the organic component is removed, porous silica or hollow silica spheres are formed.[9,11] These composite particles may also contain dopants such as organic dye molecules which are incorporated by either covalent bonding of the dye to the matrix[12] or by physical entrapment.[13]

Here we present a novel method for a one-step preparation of monodispersed bicontinuous intermingled silica/polystyrene (PS) composite particles, based on sol−gel chemistry. Specifically, we dissolve PS of various molecular weights (neat or in toulene solution; *not* Latex particles) in tetraethoxysilane (TEOS), emulsify it in a basic ethanolic solution (a Stober-type solution[14]), and stabilize the emulsion by the nonionic surfactant Triton X-100. Along with the advantage of being a simple one-step procedure which is carried out at ambient temper-

* To whom correspondence should be addressed. E-mail: david@chem.ch.huji.ac.il.

(1) Antonietti, M.; Berton, B.; Goltner, C.; Hentze, H. P. *Adv. Mater.* **1998**, *10*, 154. Mecking, S.; Thomann, R. *Adv. Mater.* **2000**, *12*, 953.
(2) Honda, F.; Honda, H.; Koishi, M.; Matsuno, T. *J. Chromatogr.* **1997**, *775*, 13. Bottoli, C. B. G.; Chaudhry, Z. F.; Fonseca, D. A.; Collins, K. E.; Collins, C. H. *J. Chromatogr.* **2002**, *948*, 121. Goworek, J.; Derylo-Marczewska, A.; Stefaniak, W.; Zgrakja, W.; Kusak, R. *Mater. Chem. Phys.* **2002**, *77*, 276.
(3) Velev, O. D.; Furusawa, K.; Nagayama, K. *Langmuir* **1996**, *12*, 2374.
(4) Xu, X.; Friedman, G.; Humfeld, K. D.; Majetich, S. A.; Asher. S. A. *Chem. Mater.* **2001**, *14*, 1249. Lal, M.; Levy, L.; Kim, K. S.; He, G. S.; Wang, X.; Min, Y. H.; Pakatchi, S.; Prasad, P. N. *Chem. Mater.* **2000**, *12*, 2632. Amalvy, J. I.; Percy, M. J.; Armes, S. P. *Langmuir* **2001**, *17*, 4770.
(5) Petrovicova, E.; Knight, R.; Schadler, L. S.; Twardowski, T. E. *J. Appl. Polym. Sci.* **2000**, *77*, 1684. Mousa, W. F.; Kobayashi, M.; Kitamura, Y.; Zeineldin, I. A.; Nakamura, T. *J. Bio. Mater. Res.* **1999**, *47*, 336. Br'chet, Y. J.-Y.; Cavaill, J.-Y.; Chabert, E.; Chazeau, L.; Dendievel, R.; Flandin, L.; Gauthier, C. *Adv. Eng. Mater.* **2001**, *3*, 571. Bokobza, L.; Garanaud, G.; Mark, J.; Jethmalani, J. M.; Seabolt, E. E.; Ford, W. T. *Chem. Mater.* **2002**, *14*, 162.
(6) Pastoriza-Santos, I.; Scholer, B.; Caruso, F. *Adv. Funct. Mater.* **2001**, *11*, 122. Caruso, F. *Adv. Mater.* **2001**, *13*, 11.
(7) Tissot, I.; Novat, C.; Lefebvre, F.; Bourgeat-Lami, E. *Macromolecules* **2001**, *17*, 5737.
(8) Barthet, C.; Hickey, A. J.; Cairns, D. B.; Armes, S. P. *Adv. Mater.* **1999**, *11*, 408. Bourgeat-Lami, E.; Lang, J. *J. Colloid Interface Sci.* **1998**, *197*, 293. Mandal, T. K.; Fleming, S.; Walt, D. R. *Chem. Mater.* **2000**, *12*, 3481. Putlitz, B.; Landfester, K.; Fischer, H.; Antonietti, M. *Adv. Mater.* **2001**, *13*, 500. Luna-Xavier, J.-L.; Bourgeat-Lami, E.; Guyot. A. *Colloid Polym. Sci.* **2001**, *279*, 947. Antonietti, M.; Landfester, K. *Prog. Polym. Sci.* **2002**, 689.
(9) Iskandar, F.; Mikrajuddin, O. K. *Nano Lett.* **2001**, *1*, 231.
(10) Fleming, M. S.; Mandal, T. K.; Walt, D. R. *Chem. Mater.* **2001**, *13*, 2210.
(11) Caruso, F.; Caruso, R. A.; Möhwald, H. *Science* **1998**, *282*, 1111. Zhong, Z.; Yin, Y.; Gates, B.; Xia, Y. *Adv. Mater.* **2000**, *12*, 206.
(12) Van Blaaderen, A.; Varij, A. *Langmuir* **1992**, *8*, 2921. Imhof, A.; Megens, M.; Engelberts, J. J.; De Lang, D. T. N.; Sprik, R.; Vos, W. L. *J. Phys. Chem. B* **1999**, *103*, 1408. Nyffenegger, R.; Quellet, C.; Ricka, J. *J. Colloid Interface Sci.* **1993**, *159*, 150. Graf, C.; Schärtl, W.; Fischer, K.; Hugenberg, N.; Schmidt, M. *Langmuir* **1999**, *15*, 6170.
(13) Shibata, S.; Taniguchi, T.; Yano, T.; Yasumori, A.; Yamane, M. *J. Sol−Gel. Sci. Technol.* **1994**, *2*, 755. Shibata, S.; Taniguchi, T.; Yano, T.; Yamane, M. *J. Sol−Gel. Sci. Technol.* **1997**, *10*, 263.
(14) Stober, W.; Fink, A. *J. Colloid Interface Sci.* **1968**, *26*, 62.

10.1021/cm020980h CCC: $25.00
Published on Web 03/22/2003

Table 1. Compositions Tested for Particle Preparations

sample	polymer	amount (g)	TEOS amount (mL)	surfactant	solvent
PS/Si-1	PS 10000	0.2	2	Triton X-100	none
PS/Si-2	PS 10000	0.5	2	Triton X-100	toluene 3 mL
PS/Si-3	PS 50000	0.2	2	Triton X-100	toluene 3 mL
PS/Si-4	PS 150000	0.1	2	Triton X-100	toluene 2 mL
PS/Si-5	PS 10000	0.3	2	Triton X-100	none
PS/Si-6	PS 10000	0.2	2	CTAB[a]	none
PS/Si-7	PS 10000	0.2	2	SDS[a]	none
PS/Si-8	PS 10000	0.2	2	none[a]	none
PS/Si-9	PS 10000	0.2	1	Triton X-100	none
PS/Si-10	PS 10000	0.2	1	Triton X-100	toluene 0.5 mL

[a] Particles are not obtained under these conditions.

atures, good monodispersion of the particles is obtained, host molecules can be entrapped, porous silica particles can be obtained by total removal of the PS phase, and core−shell architecture is obtained by its partial removal. These features, as well as particle characterization by a variety of methods, are described next.

2. Experimental Details

Chemicals. TEOS 98%, Nile blue A, Sudan IV, Sudan III, sodium dodecyl sulfate (SDS), and cetyltrimethylammonium bromide (CTAB) were all from Aldrich. Triton X-100 was from BDH. Polystyrene monohydroxy terminated MW 10 000 (PS-10,000), PS monocarboxy terminated MW 50 000 (PS-50,000), and PS monocarboxy terminated MW 150 000 (PS-150,000) were from Scientific Polymer Products Inc.

Particles Preparation. In a typical procedure, 0.5 or 0.2 g of the polymer (PS-10,000 or PS-50,000; PS/Si-2 and PS/Si-3, Table 1) was dissolved in 3.0 mL of toluene, then various amount of TEOS (typically 2.0 mL) and 0.4 g of Triton X-100 were added to the toluene solution. In a 100-mL Erlenmeyer flask, 50 mL of ethanol was stirred with 10 mL of ammonium hydroxide ~25% (NH_3 by weight). The toluene/TEOS polymer solution was then poured into the basic ethanol solution and stirred for 24 h. Centrifuging for 10 min at 6000 rpm cleaned the resulting particle dispersion. The white precipitate was separated and then re-dispersed in water or ethanol.

Two additional variations on this procedure were tested: (A) A 0.2-g aliquot of PS-10,000 was dissolved in 2.0 mL of TEOS by sonication (10 min) leading to PS/Si-1; or in 1.0 mL of TEOS, leading to PS/Si-9, employing in both cases the above procedure. (B) In the case of PS-150000 (PS/Si-4), which is not well-dissolved in TEOS, 0.1 g of the polymer was dissolved in 5.0 mL of toluene and 2.0 mL of TEOS, and the surfactant was added to the basic ethanolic solution (see Table 1 for other compositions). Our lead preparation procedures for the majority of the experiments and tests were those for PS/Si-1 and PS/Si-2, Table 1.

Neither the anionic surfactant SDS (sample PS/Si-7, Table 1) nor the cationic CTAB (sample PS/Si-6, Table 1), which were tested as replacement surfactants for Triton X-100, could affect particle formation in the case of PS-10,000. Removal of the surfactant altogether was tested as well (sample PS/Si-8): When the PS-10,000/TEOS solution was added dropwise to the basic ethanol solution under stirring, an emulsion was obtained but TEM revealed only a low quantity of particles.

Dye Entrapments. A 0.05-g portion of the hydrophobic Sudan III (1.42×10^{-4} mol) or Sudan IV (1.3×10^{-4} mol) were dissolved in the TEOS phase for the entrapment in PS-10,000 or in toluene for entrapment in PS-150,000, and the particles were prepared as described above for sample PS/Si-5. Hydrophilic dye Nile blue A (0.04 g; 5.4×10^{-5} mol) was dissolved in the basic ethanol solution under stirring and particles were prepared by the same procedure.

Hydrophobic Phase Extraction. The extraction of PS from the composite particles was performed in two ways: (i) Extraction with methylene chloride in a Soxhlet extractor for 12 h (PS/Si-1, PS/Si-2, and PS/Si-4). The methylene chloride phase was checked qualitatively with ethanol for existence of the PS (PS precipitates by adding ethanol solution). (ii) Calcinations were carried out by spreading the samples (PS/Si-1 or PS/Si-2) on glass slides or aluminum foil and heating at 500 °C for 5 h.

Particle Characterization and Instrumentation. Transmission electron microscopy (TEM) observations were performed on a JEOL 100 CX microscope operating at 80 kV, and on a Philips CM 12 microscope operating at 120 or 100 kV. Samples for TEM observations were prepared by deposition of the aqueous or ethanolic dispersions on Formvar/Carbon 300 mesh copper grid. The dispersions were air-dried for 1 min, and the extra solution was blotted off. X-ray photoelectron spectroscopy (XPS) measurements were performed in UHV (2.5×10^{-10} Torr base pressure) using a 5600 Multi-Technique System (PHI). The samples were irradiated with an Al Kα monochromatic source (1486.6 eV) and the emitted electrons were analyzed by a spherical capacitor analyzer using a slit aperture of 0.4 mm. Analysis was carried out at the surface and after sputtering with the 4 kV Ar^+ ion gun. High-resolution measurements were performed at pass energy of 11.75 eV with 0.025 eV/step interval. The surface of the samples was positively charged during measurements. Using a charge neutralizer compensated this charging. Surface area and porosity measurements of the dried powders (all samples were dried at 100 °C under vacuum overnight until the pressure stabilized at about 3 μm Hg) were determined from nitrogen adsorption/desorption isotherms using a Micromeritics ASAP 2000 instrument, employing the BET equation for surface area computation and the BJH approach for pore size analysis. IR measurements were carried out on a Bruker Vector 22 spectrometer. The samples were prepared in KBr pellets. UV measurements were carried out on a HP-8453 spectrophotometer using 2-mm quartz cuvettes. Differential scanning calorimetric (DSC) analysis was preformed on a Mettler DSC822^e at the heating rate of 10 °C/min under nitrogen. Thermogravimetric analysis (TGA) was preformed on a Mettler TG-50 system at 10 °C/min.

3. Results and Interpretations

TEM Observations. As seen in Figure 1, the composite particles are obtained in a monomodal distribution (note the hexagonal packing zones). It is also seen that the particles have a smooth surface and that they are discrete and nonaggregated. (Figures in this report are of various representative examples from Table 1). Average particle sizes are all around half a micron or less (e.g., 530 nm for PS/Si-2 (see Table 1 for details), 350 nm for PS/Si-3, and 450 nm for PS/Si-4).

Well-defined particles were obtained only with the nonionic surfactant Triton X-100. Particles are not obtained, as mentioned above, with either the anionic SDS or with the cationic surfactant CTAB, or in the absence of Triton X-100 (Table 1). That only the nonionic surfactant affects particle formation in ethanolic system

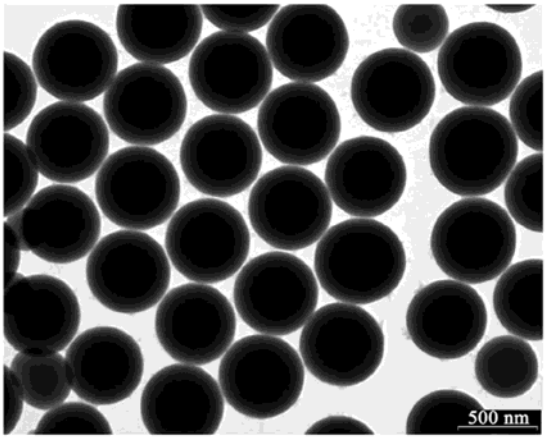

Figure 1. Composite sol−gel particles of polystyrene (of molecular weight 10,000) and silica (shown is sample PS/Si-2, Table 1). Average particle size: 530 nm.

is understood from its structure, namely the relatively long hydrophilic chains of N = 9 or 10 $-CH_2O-$ units, and a short bulky hydrophobic head.

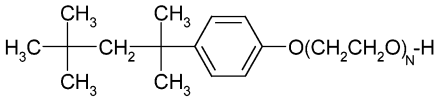

Thus, at first, the hydrophobic head dissolves well within the interface of the hydrophobic droplet, which is composed of the PS chains, TEOS molecules, and toluene (optional), and stabilizes the micellar structure, out of which extend the long $-CH_2O-$ residues. Water molecules are entangled within the $-CH_2O-$ layer, which serves as the zone into which TEOS molecules diffuse and begin to form the silica phase. The forming silica phase then absorbs more water molecules that reach the hydrophobic core, and so on. We believe, therefore, that the necessary feature of the surfactant is in providing a substantial layer within which the sol−gel process begins to take place. As we shall see below, the particle architecture as a whole is not that of a core−shell but of a true composite of silica and PS. This indicates that the penetration of water is efficient and that the process of sol−gel silica matrix formation is fast, not allowing the PS molecules to form a phase; and it indicates that the forming silica efficiently transports water molecules to the TEOS molecules which solvate the PS chains.

The composite PS/silica particles were also examined by TEM after calcination at 500 °C for 5 h and after extraction in methylene chloride (see Experimental Details). The resulting SiO_2 particles are not hollow but full as seen in Figure 2 and as confirmed by gray-scale analysis. When the polymer is removed from the composite particles by partial extraction one obtains core shell architecture (Figure 3), in which the shell is porous silica, and the core is the PS/SiO_2 composite. The relative thickness of the two phases can be controlled by the duration of the extraction.

IR Observations. Proof of the composite nature of the particles and of the ability to remove the PS phase was provided by FTIR spectra, as shown in Figure 4. The typical PS absorption bands at 1451, 1491, 1600, 2919, and 3022 cm^{-1} (Figure 4a) are clearly seen in the spectrum of the composite particles (Figure 4b), which

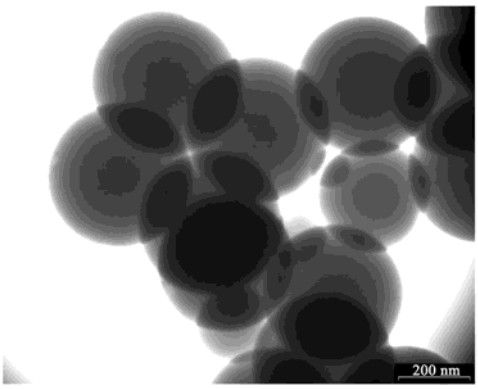

Figure 2. Porous silica particles produced after calcination of the composite particles (shown for PS/Si-2).

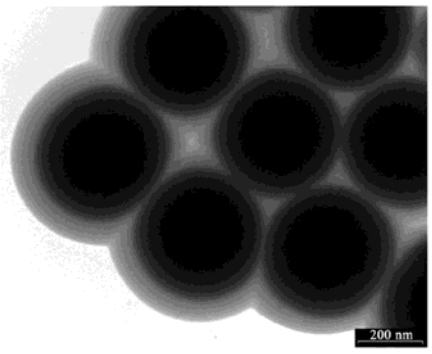

Figure 3. SiO_2-shell/(PS+SiO_2)-core architecture is achieved by partial extraction of the hydrophobic phase from the composite particles (shown is the silica-rich composition PS/Si-1 (Table 1)).

displays also the typical silica absorption bands at 1111 cm^{-1} (the asymmetrical stretching of the siloxane bond Si−O−Si) and at 941 cm^{-1} and 3430 cm^{-1} (the stretching of the hydroxyl group in Si−OH and of residual water). These silica peaks are also seen in the spectrum of the particles after the above-described extraction (Figure 4c), where it is evident that the PS absorption bands have disappeared. (The peaks at 1385 and 1401 cm^{-1} indicate the existence of residual unhydrolyzed $SiOCH_2CH_3$ (the CH_2 and CH_3 groups, respectively);[15] and the peak at 1640 cm^{-1} is of adsorbed water[16]).

XPS Measurements and Depth Profiling. High-resolution XPS measurements (Figure 5) indicated the composite nature of the particles. That the surface of the composite particles contains silica was evident from the 103.7 eV (Si2p) and 533.2 eV (O1s) peaks;[17] and the PS at the interface is clearly seen through the 284.4 eV C1s peak and through the characteristic $\pi-\pi^*$ shake-up satellite peak of the phenyl rings, between 290 and 292 eV.[18] It should be noted that this shake-up sattelite is seen for the PS-rich samples (shown in Figure 5), but

(15) Tejedor-Tejedor, M. I.; Paredes, L.; Anderson, M. A. *Chem. Mater.* **1998**, *10*, 3410.
(16) Schlottig, F.; Textor, M.; Georgi, U.; Rower, G. *J. Mater. Sci. Lett.* **1999**, *18*, 599.
(17) Gallas, B.; Kao, C.-C.; Fisson, S.; Vuye, G.; Rivory, J.; Bernard, Y.; Belouet, C. *Appl. Surf. Sci.* **2002**, *185*, 317; Dos Santos, J. H. Z.; Ban, H. T.; Teranishi, T.; Uozumi, T.; Sano, T.; Soga, K. *Appl. Catal. A.* **2001**, *220*, 287.
(18) Beamson, G., Briggs, D. *High-Resolution XPS of Organic Polymers The Scienta ESCA300 Database*; John Wiley and Sons: Chichester, U.K., 1992. France, M. R.; Short, R. D. *Langmuir* **1998**, *14*, 4827. Idage, S. B.; Badrinarayan, S. *Langmuir* **1998**, *14*, 2780.

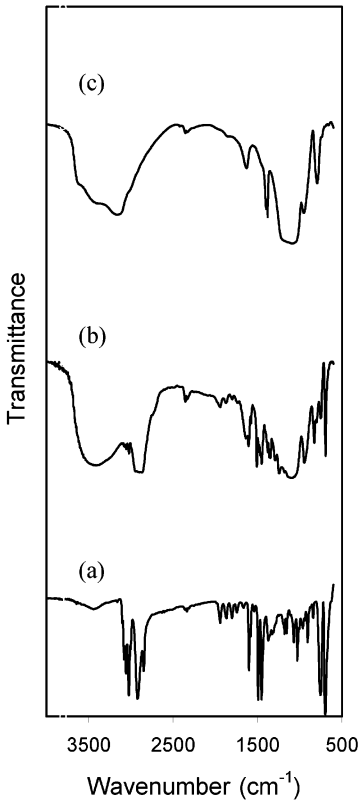

Figure 4. FTIR spectra of (a) polystyrene 10,000; (b) the PS composite particles (shown for PS/Si-1); and (c) the particles after extraction of the polystyrene phase.

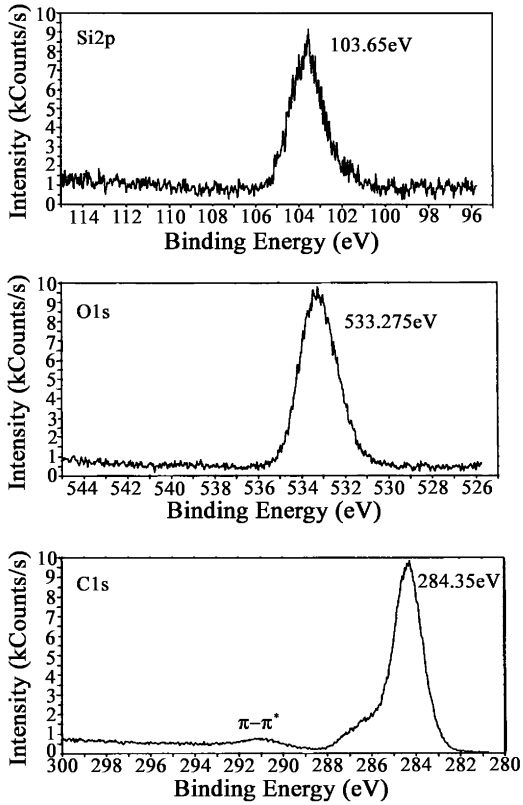

Figure 5. XPS high-resolution spectra of the composite particles (shown for the PS-rich sample PS/Si-10).

not for the silica-rich particles (such as demonstrated in Figure 3).

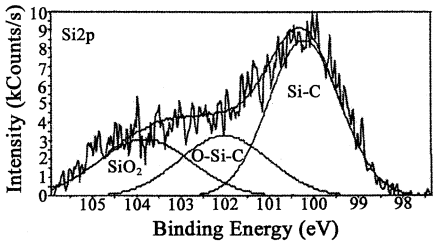

Figure 6. Deconvolution curves for Si2p after 43 min of sputtering (PS/Si-10).

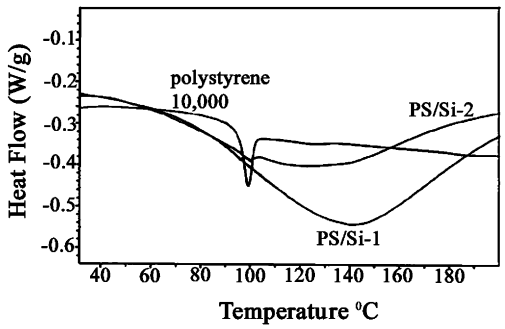

Figure 7. DSC thermograms of free polystyrene and of the composites PS/Si-1 and PS/Si-2.

Depth profiling was performed in order to characterize the internal composition of the particles. The profiling was carried out by sputtering with Ar^+ ions (Experimental Details) at a rate of 60 Å/min on an area of 300 × 300 μm. As seen in Figure 6, after 43 min of sputtering the Si(2p) peak widens and shifts to lower energies with the appearance of a tail at 100.2 eV which is indicative of the Si−C bond,[19] namely of the sputtering-induced formation of silicon carbide species. Thus, after the prolonged sputtering, 24% SiO_2, 25% Si−O−C, and 51% Si−C species are seen (Figure 6).

Thermogravimetric Analysis and Differential Scanning Calorimetry. Thermal analyses of the composite particles revealed interesting differences between the DSC thermograms as compared to those of free PS and in relation to samples with varying PS/SiO_2 composition. TGA of two samples used for the DSC analysis (Figure 7; TGA not shown) revealed a PS content of 29% (by weight) for PS/Si-1 and 49% for PS/Si-2. As can be seen in the DSC curves (Figure 7), while the free PS-10,000 melts sharply at 95 °C, the two composite samples reveal a very broad peak, the minimum of which is significantly shifted to higher temperatures of around 130 °C for the PS rich PS/Si-2 and around 143 °C for PS/Si-1. These broadening and shift indicate that the PS chains are well entangled within the silica matrix, creating a wide population of nearly molecular-level domains, each of which "melts" under the silica matrix constrains at a different (and higher than for free PS) temperature. And because in PS/Si-1 there is less PS in the same amount of silica, these effects are more pronounced than those seen for PS/Si-2. In fact, in the PS-rich sample (PS/Si-2) one can still detect a

(19) Terekhov, V. A.; Kashkarov, V. M.; Manukovskii, S. A. V.; Domasheskaya, E. P. *J. Electron. Spectrosc.* **2001**, *114*, 895. Brooks, P. N.; Fraser, S.; Short, R. D.; Hanley, L.; Fuoco, E.; Roberts, A.; Hutton, S. *J. Electron. Spectrosc.* **2001**, *121*, 281. Hijikata, Y.; Yaguchi, H.; Yoshikawa, M.; Yoshida, S. *Appl. Surf. Sci.* **2001**, *184*, 161. Volz, K.; Baba, K.; Hatada, R.; Ensinger, W. *Surf. Coat. Technol.* **2001**, *136*, 197.

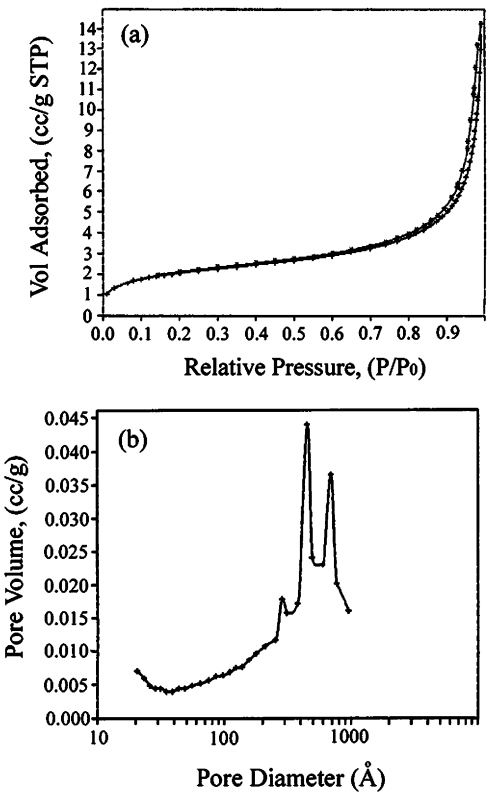

Figure 8. (a) Nitrogen BET adsorption/desorption isotherm of sample PS/Si-4 obtained after extraction of the PS phase. (b) The bimodal pore distribution of the same sample.

small peak at the original melting point, showing that the distribution of PS for this composite contains some true PS-10,000 domains. More information on this nearly molecular-level distribution was obtained from the extraction experiments results, described next.

Surface Area Measurements after Removal of the PS. Three PS-extracted samples were extracted, namely PS/Si-1, -2, and -4. All three samples showed type II isotherms (Figure 8a) indicating mesoporosity of the solids. The N_2−BET surface areas were 7.0, 16.0, and 6.4 m^2/g. The higher surface area of Si-2 compared to Si-1 reflects the 2.5-fold higher amount of PS in the former. The even-lower amount of PS-150,000 in Si-4 (Table 1) is compensated by its higher MW, and the surface area does not change significantly (6.4 m^2/g). (Prior to extraction the surface area of the nonporous particles was around 2.4 m^2/g). Interestingly, all three samples show a bimodal BJH desorption pore-volume distribution around 37 nm and around 70 nm (Figure 8b). The question is whether these pore sizes are indicative of the sizes of the PS domains. Recalling that the radius of gyration of single molecules is 16 nm for PS-150,000 and 3.2 nm for PS-10,000, one may conclude that the PS molecules are arranged in the form of only a few molecules per domain.

Entrapment of Dyes in the Composite Particles. The entrapment of the hydrophobic dye Sudan IV (Experimental Details) proved to be simple experimentally, and very efficient, and resulted in leach-proof particles. Re-dispersion of the cleaned, dried, dark red powder in water showed none of this hydrophobic molecule in solution for months. UV−vis absorption spectra (not shown) exhibited the typical 510 nm peak of the entrapped dye, which is the same wavelength as is obtained in toluene solution. This confirms that the hydrophobic dye resides inside the particle within the hydrophobic domains of polystyrene. Similar leach-proof stability was obtained for the hydrophilic cationic dye Nile blue A, which resides in the silica phase, as was indicative from the UV−vis absorption spectrum which is similar to the spectrum in water/ethanol solution. Although it is a water-soluble dye, water was unable to extract it probably because of strong ionic interaction between the negatively charged silica and the cationic dye. These direct entrapments of both hydrophobic and hydrophilic dyes are advantageous alternatives to the preparation of leach-proof dyed particles by covalent-attachment methods.

Conclusions

All of these observations indicate the formation of bicontinuous silica/PS composite particles where the PS phase has a typical domain size of several tenths of nm, composed of a few PS molecules. According to the observations, we think that the morphology of the particles is the consequence of a rapid process in which the hydrophobic TEOS molecules are converted to a rigid hydrophilic matrix which entraps the PS molecules without allowing them to arrange into large PS phases. The synthesis comprises a simple one-step room-temperature procedure and provides high yield of monodispersed spherical composite particles in the submicron range. Three useful applications of these particles were demonstrated: as a source for the formation of mesoporous silica particles; as a source for core−shell architecture, and as leach-proof carriers for dyes. These and other applications are being further developed in our laboratory.

Acknowledgment. We gratefully acknowledge support from the Ministry of Science, Art and Sport through the Tashtiot project, the Israel Science Foundation through Grant 143/00-12.0, and the Robert Szold Fund. We thank Mrs. Ruth Govrin-Lippman (Life Sciences, The Hebrew University) for the TEM measurements and Dr. Larisa Burstein (The Wolfson Center of Materials Science, Tel Aviv University) for carrying out the XPS measurements.

CM020980H